Characterization of Dominant and Recessive Assembly-defective Mutations in Mouse Neurofilament NF-M

Philip C. Wong and Don W. Cleveland

The Johns Hopkins University School of Medicine, Department of Biological Chemistry, Baltimore, Maryland 21205

Abstract. We have generated a set of amino- and carboxy-terminal deletions of the neurofilament NF-M gene and determined the molecular consequences of forced expression of these mutant constructs in mouse fibroblasts. To follow the expression of mutant NF-M subunits in transfected cells, a 12 amino acid epitope (from the human c-*myc* protein) was expressed at the carboxy terminus of each mutant. We show that NF-M molecules missing up to 90 or 70% of the nonhelical carboxy-terminal tail or amino-terminal head domains, respectively, incorporate readily into an intermediate filament network comprised either of vimentin or NF-L, whereas deletions into either the amino- or carboxy-terminal α-helical rod region generate assembly-incompetent polypeptides. Carboxy-terminal deletions into the rod domain invariably yield dominant mutants which rapidly disrupt the array of filaments comprised of NF-L or vimentin. Accumulation of these mutant NF-M subunits disrupts vimentin filament arrays even when present at ~1% the level of the wild-type subunits. In contrast, the amino-terminal deletions into the rod produce pseudo-recessive mutants that perturb the wild-type NF-L or vimentin arrays only modestly. The inability of such amino-terminal mutants to disrupt wild-type subunits defines a region near the amino-terminal α-helical rod domain (residues 75–126) that is required for the earliest steps in filament assembly.

THE eukaryotic cytoskeleton is comprised of microtubules, actin filaments and intermediate filaments (IFs)[1] that together with associated proteins localized at nuclear and plasma membrane binding sites establish the internal cytoarchitecture of most eukaryotic cells. While the dynamics and functional role of microtubules and actin filaments are well characterized, neither the assembly characteristics nor the function of IFs are firmly established (for reviews, see Klymkowsky et al., 1989; Steinert and Liem, 1990). Based on DNA sequence data and their tissue-specific expression, IFs can be subdivided into six distinct groups: vimentin (mesenchymal cells), keratins (epithelial cells, desmin (muscle cells), glial fibrillary acidic protein (glial cells), lamins (all cell types), and neurofilaments (NFs) (neuronal cells). There is no reason to believe that these comprise the entire family of IF subunits, a point underscored by the recent identification of three additional IF proteins expressed in different subsets of neurons. These include peripherin, a vimentin-like IF polypeptide expressed in a subset of peripheral neurons (Portier et al., 1984; Parysek and Goldman, 1987; Leonard et al., 1988), α-internexin, an NF-like polypeptide (Fliegner et al., 1990), and nestin, an IF protein expressed in neuroepithelial stem cells (Lendahl et al., 1990).

All cytoplasmic IFs are characterized by a highly conserved central α-helical coiled-coil domain (~310 amino acids) flanked by two nonhelical domains of variable length and sequence (Geisler and Weber, 1986; Franke, 1987). The amino- and carboxy-terminal regions play role both in end-to-end and in lateral interactions of filament assembly (Geisler and Weber, 1982; Steinert et al., 1983; Traub and Vorgias, 1983; Kaufmann et al., 1985). However, not only does one naturally occurring bovine keratin (K8) contain only a 13 amino acid tail (Bader et al., 1986), Albers and Fuchs (1987) and van den Heuvel et al. (1987) used DNA transfection to demonstrate that essentially all of the carboxy-terminal domain may be deleted for a type I keratin and for desmin, respectively, without disrupting coassembly with wild-type subunits into filaments in vivo. Recently, Albers and Fuchs (1989) have shown for one type I keratin that both the amino-terminal and carboxy-terminal domains are dispensable for coassembly with normal type I and type II keratin subunits.

Unlike most IFs, the major mammalian NFs are coassembled from three subunits: NF-L, NF-M, and NF-H, whose apparent molecular masses on SDS-PAGE gels are 68, 150, and 200 kD, respectively. The NF polypeptides differ in size mainly as the result of increasingly long carboxy-terminal extensions (Geisler et al., 1983). In NF-M and NF-H, these carboxy-terminal regions can be highly phosphorylated, a feature that in part accounts for their anomalous migration on SDS-PAGE gels (Julien and Mushynski, 1982, 1983; Carden et al., 1985). It seems likely that phosphorylation

1. *Abbreviations used in this paper*: IF, intermediate filament; MSV, murine sarcoma virus; NF, neurofilament.

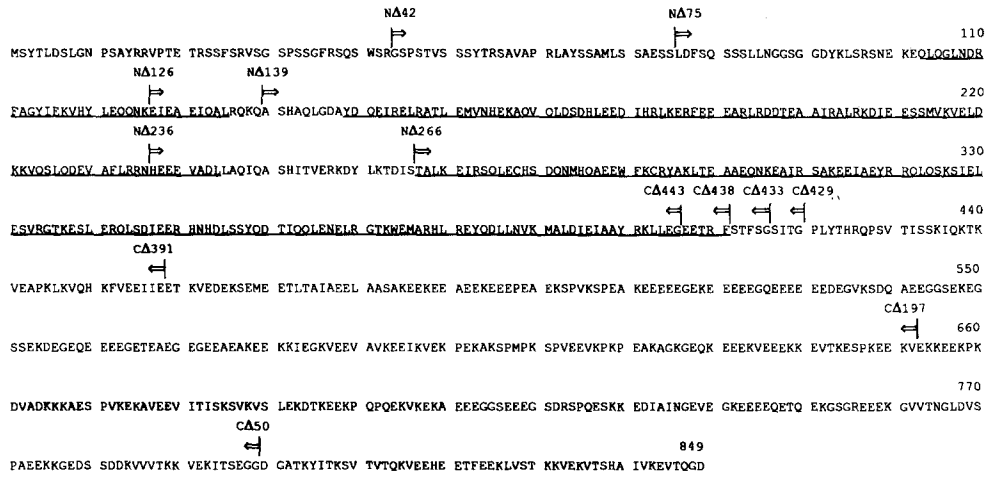

Figure 1. Positions of amino- and carboxy-terminal truncation mutants in the primary sequence of the mouse NF-M polypeptide. The one letter code has been used to display the primary sequence of the mouse NF-M polypeptide, as deduced from DNA sequencing (Levy et al., 1987). Residues within the predicted helical rod domain (Geisler et al., 1985) are underlined. Positions where amino-terminal or carboxy-terminal truncation mutants of NF-M begin or end are marked.

(especially of NF-H, which may be phosphorylated up to 50 times [Geisler and Weber, 1987; Lees et al., 1988]), may play a role in the interaction of NFs with other neuronal components (e.g., microtubules) (Julien and Mushynski, 1983; Sternberger and Sternberger, 1983; Minami and Sakai, 1985).

The organization of the three NF proteins in the native NF polymer has yet to be determined. In vitro reconstitution experiments using each of the three NF subunits first demonstrated that (*a*) NF-L can self-assemble into filaments in vitro (Geisler and Weber, 1981; Liem and Hutchinson, 1982), (*b*) that under some conditions NF-M can also self-assemble (Gardner et al., 1984; Tokutake et al., 1984), and (*c*) that NF-H is assembly incompetent, forming abortive short, curly filaments that may block filament elongation (Geisler and Weber, 1981). Antibody decoration of nervous tissue supports this view that NF-L is a component of the NF backbone, that NF-H is involved in cross-bridge formation between NFs (Hirokawa et al., 1984), and that NF-M is more closely aligned with the NF core than is NF-H (Sharp et al., 1982; Hirokawa et al., 1984). While NF-M and NF-H may well be involved in cross-bridge formation, determination of the sequences for NF-M (Geisler et al., 1984; Myers et al., 1987; Levy et al., 1987; Napolitano et al., 1987) and NF-H (Lees et al., 1988; Julien et al., 1987) revealed that each carries the conserved ≈310 amino acid rod domain. It thus seems likely that each is an integral filament subunit.

In this and the companion paper (Gill et al., 1990), we have extended our earlier study of the assembly properties of NF proteins (Monteiro and Cleveland, 1989) by the construction and analysis of a series of deletions that truncate the carboxy- or amino-terminal domains of NF-L (Gill et al., 1990) and NF-M (this paper). These latter experiments define the portion of the NF-M polypeptide that is necessary for assembly into a normal IF network and identify a series of dominant mutants that disrupt IF arrays assembled from wild-type vimentin or NF-L even when the mutant is present in very low relative amounts.

Materials and Methods

Construction of Carboxy-Terminal Deletions of NF-M

The construction of the parental plasmid pMSV-NF-M that was used for generating the set of carboxy-terminal deletions was reported earlier (see Fig. 2 and Monteiro and Cleveland, 1989). This plasmid contains the complete mouse NF-M gene linked to the murine sarcoma virus (MSV) long terminal repeat. To generate a set of carboxy-terminal deletions of NF-M, pMSV-NF-M was digested at the Nco I site located 3′ to the site of polyadenylation, followed by treatment with exonuclease III. After creating blunt-ended molecules with mung bean nuclease, the fragments were cleaved at the unique Bam HI site at the 3′ end of the NF-M gene and the resulting Bam HI–blunt-ended fragments were gel purified. A *myc*-tag cassette containing a 12 amino acid epitope from the human c-*myc* protein (see Munro and Pelham, 1987) was synthesized and ligated just 5′ to the complete 3′ untranslated and 3′ flanking sequences of the NF-L gene to create pMYC-0 (Fig. 2 *B*). pMYC-0 was linearized first with Sal I, blunted (with Klenow fragment), and cleaved with Bam HI. This fragment was gel purified and ligated to the set of pMSV-NF-M deletions, producing the desired constructs, pNFM-CΔ*x*, where *x* denotes the number of amino acids removed from the carboxy terminus of NF-M (see Fig. 2 *C*).

Construction of Amino-Terminal Deletions of NF-M

The plasmid, pNFM-CΔ50 (see Fig. 2 *C*) was chosen as the starting construct for the generation of amino-terminal deletions of NF-M. This gene encodes a nearly wild-type NF-M subunit except that the last 50 carboxy-terminal amino acids have been replaced with the 12 amino acid epitope of the human c-*myc* protein. pNFM-CΔ50 DNA was linearized at the site Cla I positioned near the 5′ end of MSV-LTR, and a set of amino-terminal deletions was generated using exonuclease III and mung bean nuclease. The blunt-ended fragments were then excised by digestion at the unique Bam HI site and the resulting Bam HI blunt-ended molecules were gel purified.

To ensure that each construct retained an appropriate 5′ untranslated region and an ATG translation initiation codon, a cassette (pNF5-ATG) was constructed to contain 23 bp of the 5′ untranslated region of the mouse NF-L gene including the coding sequences for the first two amino acids (Fig. 7 *B*). pNF5-ATG was linearized with Sal I, blunted (with mung bean nuclease), and cut at the unique Bam HI site. This fragment was gel purified, subsequently ligated to the set of pNFM-CΔ50 derivatives, and transformed into *Escherichia coli* strain DH1 to yield the final pNFM-NΔ*y* constructs shown in Fig. 7 *C*, where *y* represents the number of amino acids deleted from the amino terminus of NF-M.

Plasmid DNA from the pNFM-CΔ*x* and pNFM-NΔ*y* series were partially sequenced by the dideoxy-chain termination method to determine the deletion end points and to identify those that were linked in the correct translational reading frame to the myc tag.

Construction of NF-M Mutants Deleted in Both Head and Tail Domains

To construct an NF-M gene lacking both head and tail domains, pNFM-CΔ391 DNA was excised with Cla I and Sac II and the 6.2-kb vector-containing fragment (missing 391 residues of the carboxy-tail domain) was gel purified. The small Cla I/Sac II fragments of either pNFM-NΔ42 and pNFM-NΔ75 (containing portions of the amino-head domain) were also gel purified. The Cla I/Sac II fragment from pNFM-CΔ391 was then ligated

to the Cla I/Sac II fragments of either pNFM-NΔ42 or pNFM-NΔ75 to generate pNFM-NΔ42/CΔ391 or pNFM-NΔ75/CΔ391, respectively.

Construction of Expression Plasmids Containing Sequences Encoding the myc tag Fused to the Bacterial Gene trpE

To construct a chimeric gene that expresses the 12 amino acid myc epitope as a fusion with the bacterial protein *trpE* protein, the insert from pMYC-0 (Fig. 2 *B*) was ligated in the correct orientation into the unique Hind III site of the *trp*E gene in pATH2 (kindly provided by Dr. T. J. Koerner, Duke University, Durham, NC) and transformed into *E. coli* strain DH1. The resultant fusion protein contained an amino-terminal 32 kD of the bacterial protein *trp*E linked to the 12 amino acid myc epitope. The fusion protein was induced with indoleacrylic acid and analyzed as previously described (Lopata and Cleveland, 1987). Inspection of Coomassie blue-stained gels of extracts of induced bacteria revealed induction of a distinct 33 kD *trpE-myc* fusion polypeptide. By comparing the intensity of staining of this band in known volumes of extract with a twofold dilution series of known amounts of purified bovine albumin (from a solution whose concentration was determined by absorbance: A_{280} [1 mg/ml] = 0.67), the concentration of *trpE-myc* fusion protein (in μg/ml) in the extract was calculated.

Tissue Culture and DNA Transfection

Mouse fibroblast L cells and an L cell line stably expressing a transfected NF-L gene (MSV-NF9; Monteiro and Cleveland, 1989) were maintained in DME medium supplemented with 10% fetal bovine serum. Cells were transiently transfected using the DEAE-dextran method followed 4 h later by a dimethyl sulfoxide treatment (Lopata et al., 1984). Cells were usually analyzed 40 h posttransfection.

Stable cell lines were obtained by co-transfecting mouse L cells with a 10:1 mixture of the plasmid of interest and pSV2-neo (10 μg of DNA per 100-mm dish of cells) using lipofectin (Bethesda Research Laboratories, Gaithersburg, MD) according to a protocol described by the supplier. Colonies that were resistant to 400 μg/ml G418 (Gibco Laboratories, Grand Island, NY) were selected and positive stable cell lines were maintained in DME medium supplemented with 10% fetal calf serum and G418.

SDS Gel Electrophoresis and Immunoblotting

Cells were usually harvested 40 h after transient transfection, lysed in 0.5% (wt/vol) SDS, 50 mM Tris-Cl, pH 6.8, and the lysates were boiled in the presence of 2% β-mercaptoethanol. Protein concentrations were measured with the bicinchoninic acid method (Smith et al., 1985) and equal amounts of extracts of total cell proteins were separated by electrophoresis on 8.5% polyacrylamide gels (Laemmli, 1970), transferred onto nitrocellulose filters (type BA83; Schleicher & Schuell, Inc., Keene, NH), and immunoblotted as described (Lopata and Cleveland, 1987). To detect mutant NF-M polypeptides tagged with the myc epitope, the filters were incubated with a mouse monoclonal anti-myc antibody Mycl-9E10 (used at 1:100 of a partially purified culture supernatant; Evan et al., 1985), followed by ^{125}I-labeled sheep anti-mouse antibody (Amersham Corp., Arlington Heights, IL). For vimentin, a goat polyclonal anti-vimentin antibody (ICN ImmunoBiologicals, Costa Mesa, CA) was used (at 1:400) followed by a rabbit anti-goat IgG (Cappell Laboratories, Malvern, PA) and ^{125}I-labeled protein A.

To do quantitative immunoblotting of the amount of myc-tagged polypeptide accumulated in any sample, a series of twofold dilutions of a bacterial extract containing a known amount of *trpE-myc* fusion protein was immunoblotted in parallel with the samples of interest. By densitometric scanning of the signals on the resultant autoradiograph, a standard curve was constructed and the amount of myc tagged protein (in micrograms) present in each experimental sample was determined, after correcting for the differences in molecular weight between the *trpE-myc* fusion and the *NF-M/myc* tagged polypeptides. (Since each *trpE-myc* molecule and each NF-M tagged molecule carry one copy of the myc tag, to convert from microgram of *trpE-myc* to the equivalent microgram of NF-M tagged subunits, we multiplied by (molecular weight of the *NF-M/myc* tagged polypeptide)/(molecular weight of the *trpE-myc* polypeptide)).

Immunofluorescence Staining

Cells grown on glass coverslips were immersed for 30 s at room temperature in stabilization buffer (4 M glycerol, 100 mM Pipes, pH 6.9 and 1 mM EGTA), extracted for 30 s in stabilization buffer containing 0.5% (wt/vol) Triton X-100 at room temperature (Monteiro and Cleveland, 1989). After repeating the first wash, the samples were fixed in −20°C methanol for 5 min. The samples were rehydrated in PBS and incubated with an antibody solution (diluted in PBS containing 1% nonfat dry milk) for 1 h at room temperature. The coverslips were washed in PBS, incubated for 1 h in secondary antibody, washed again in PBS, and mounted on glass slides using Aqua-mount (Lerner Laboratories, New Haven, CT). Cells were examined on an Olympus BH-2 microscope using epifluorescence optics and photographed on Kodak TMAX film. Primary antibodies used were a mouse monoclonal antibody (Mycl-9E10; Evan et al., 1985) against the myc tag (used as a partially concentrated culture supernatant), a goat polyclonal antibody to vimentin (used at 1:40), and a rabbit polyclonal antibody to NF-L (used at 1:500; the kind gift of Dr. G. Shaw [University of Florida, Gainesville, FL]). Affinity-purified fluorescein- and rhodamine-conjugated antibodies specific for each of the primary antibodies were each used at 1:40 (obtained from ICN ImmunoBiologicals).

Results

Expression of Carboxy-Terminal Deletion Constructs in Mouse Fibroblasts

Like other IF polypeptides, NF-M is comprised of three domains: a 103 amino acid head domain, a 308 amino acid helical domain (using the borders proposed by Geisler et al. [1985]), and a 438 amino acid carboxy-terminal tail (the sequence of the domains is shown in Fig. 1). To investigate the assembly properties of the NF-M polypeptide, we initially generated a set of carboxy-terminal deletion mutants starting from a mouse NF-M gene in which the presumptive transcriptional promoter was replaced with the strong promoter of MSV (Fig. 2 *A*). We have previously shown that this promoter is highly active in mouse L cells (Monteiro and Cleveland, 1989). To facilitate the detection of the product encoded by each mutant gene, we fused a 12 amino acid

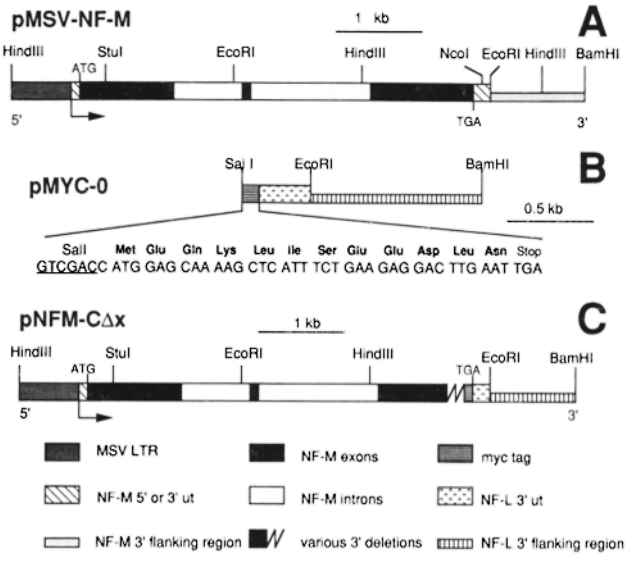

Figure 2. Gene constructs for expression of carboxy-terminal truncations of NF-M. (*A*) Schematic drawing of the MSV-NF-M gene. (*B*) Schematic of pMYC-0, which carries the sequences encoding the 12 amino acid c-myc tag (Evan et al., 1985) followed by a TGA stop codon and the 3′ untranslated and 3′ flanking regions of the mouse NF-L gene. (*C*) Schematic of the pNFM-CΔ*x* series of genes deleted to varying extents into the carboxy-terminal coding sequence of NF-M.

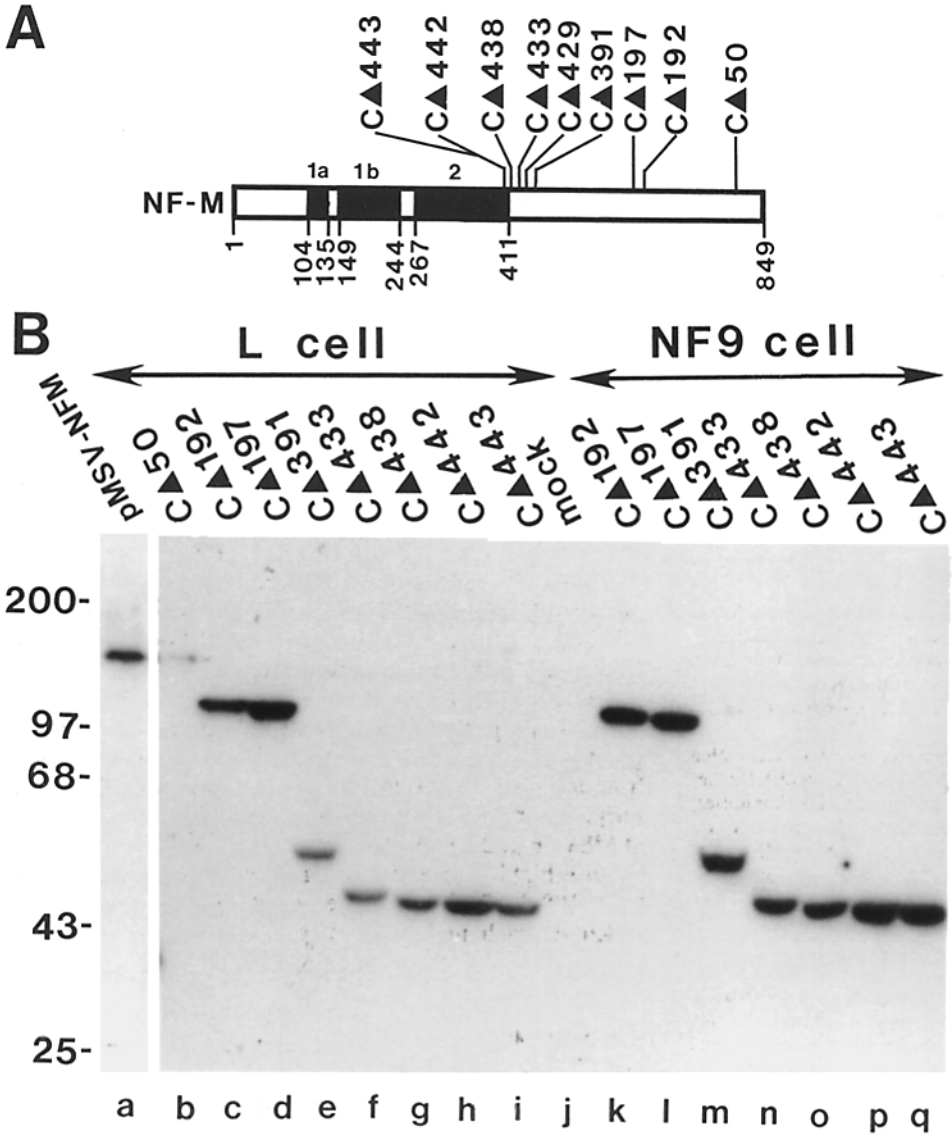

Figure 3. Immunoblot detection of carboxy-terminal mutant polypeptides accumulated following transient transfection of pNFM-CΔ*x* constructs into either mouse L cells or MSV-NF9 cells. (*A*) Schematic drawing of the NF-M polypeptide. The helical domain is represented by the closed rectangles and the deletion endpoints of specific mutants are indicated. (*B*) Immunoblot detection of NF-M polypeptides accumulated 40 h after transfection. Total extracts of cellular proteins (50 μg per extract) from cells transfected with each mutant were analyzed by immunoblotting. NF-M wild-type and mutant polypeptides were detected using an anti-NF-M antibody or using an anti-myc-tag antibody, respectively. Lane *a*, protein extract from L cells transfected with pMSV-NF-M DNA; lanes *b–i*, protein extracts from L cells transfected with the corresponding pNFM-CΔ*x* DNAs as indicated; lane *j*, protein extract from L cell transfected with pUC19 DNA; lanes *k–q*, protein extracts from MSV-NF9 cells transfected with the respective pNFM-CΔ*x* DNAs. Molecular mass markers (in kilodaltons) are indicated at the left.

segment (from the human c-*myc* protein) to the carboxy terminus of each mutant (see Fig. 2, *B* and *C*). This segment of c-*myc* was chosen as a tag because a monoclonal antibody (Evan et al., 1985) that recognizes this epitope on the human c-*myc* (but not mouse c-*myc*) was available. The deletion end-point of each mutant was determined by DNA sequencing and constructs in which the NF-M and tag sequences were linked in a continuous reading frame were selected for analysis (Fig. 3 *A*). Each mutant construct is denoted by pNFM-CΔ*x*, where *x* refers to the number of amino acids removed from the carboxy terminus of NF-M (the precise positions of the deletion end points are marked on the NF-M sequence presented in Fig. 1).

The deletion constructs were transfected into mouse L cells that normally express vimentin, and total cellular proteins were extracted 40 h posttransfection. Protein samples were resolved by SDS-PAGE and analyzed by immunoblotting using the specific monoclonal antibody that binds to the 12 amino acid myc tag. As shown in Fig. 3 *B* (lanes *b–i*), a myc-tagged protein band was detected in extracts from cells transfected with each mutant and the sizes were consistent with that predicted on the basis of sequence analysis. By

Figure 4. NF-M molecules missing up to 90% of the nonhelical carboxy-tail domain incorporate readily into the vimentin network of L cells, whereas deletions near to the carboxy-terminal helical domain disrupt assembly of the vimentin array. Mouse L cells grown on coverslips were transfected with plasmids pNFM-CΔ50 (*A* and *B*), pNFM-CΔ391 (*C* and *D*), pNFM-CΔ429 (*E* and *F*), or pNFM-CΔ443 (*G* and *H*). (*A*, *C*, *E*, and *G*) The mutant NF-M polypeptides were visualized 40 h after transfection using Mycl-9E10 monoclonal antibody (that recognizes the carboxy-terminal myc tag) followed by fluorescein-conjugated rabbit anti-mouse IgG; (*B*, *D*, *F*, and *H*) vimentin was visualized in the same transfected cells using double immunofluorescence with a goat polyclonal vimentin antibody followed by a rhodamine-conjugated rabbit anti-goat IgG. Bar, 10 μm.

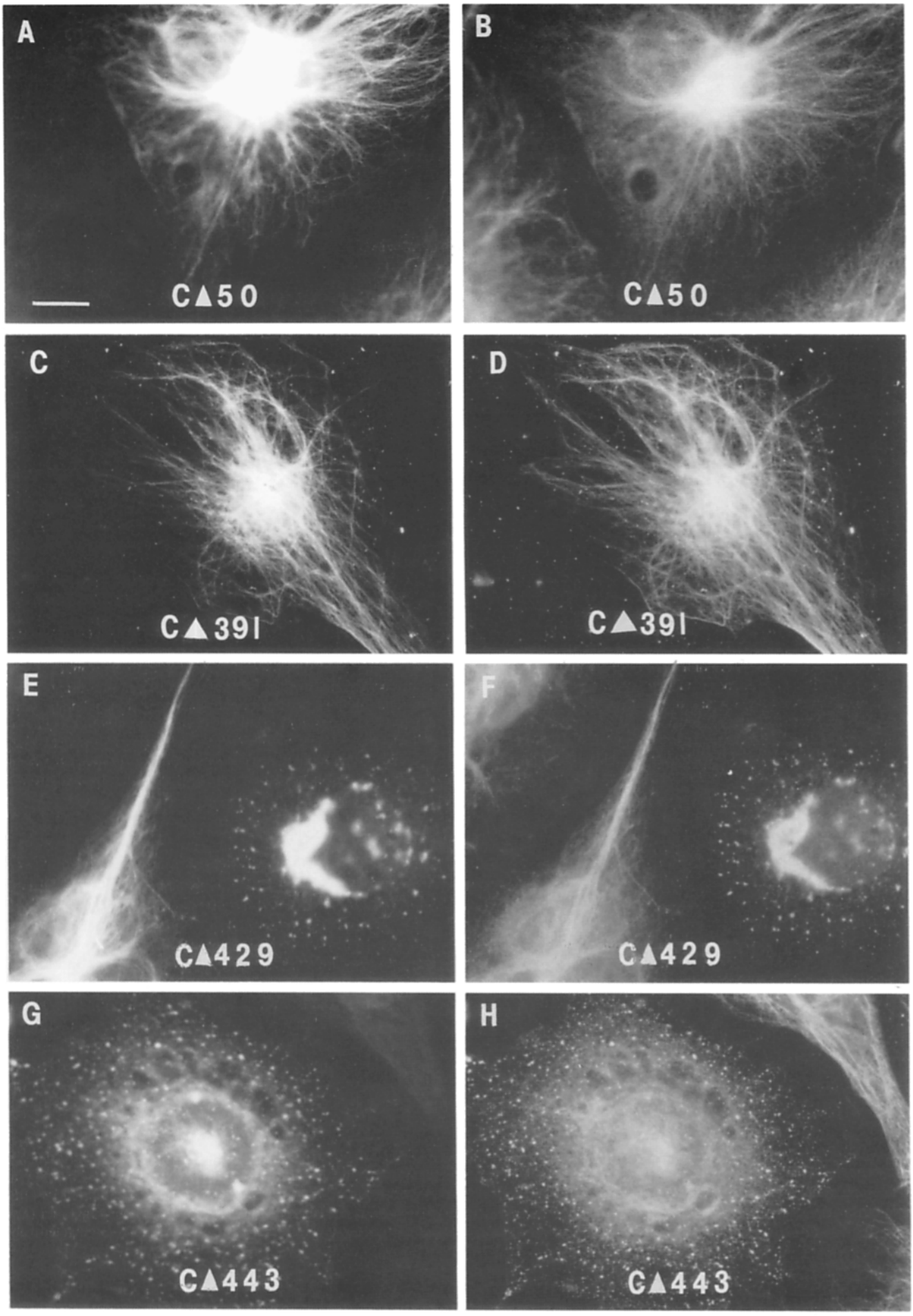
A
CΔ50
B
CΔ50
C
CΔ391
D
CΔ391
E
CΔ429
F
CΔ429
G
CΔ443
H
CΔ443

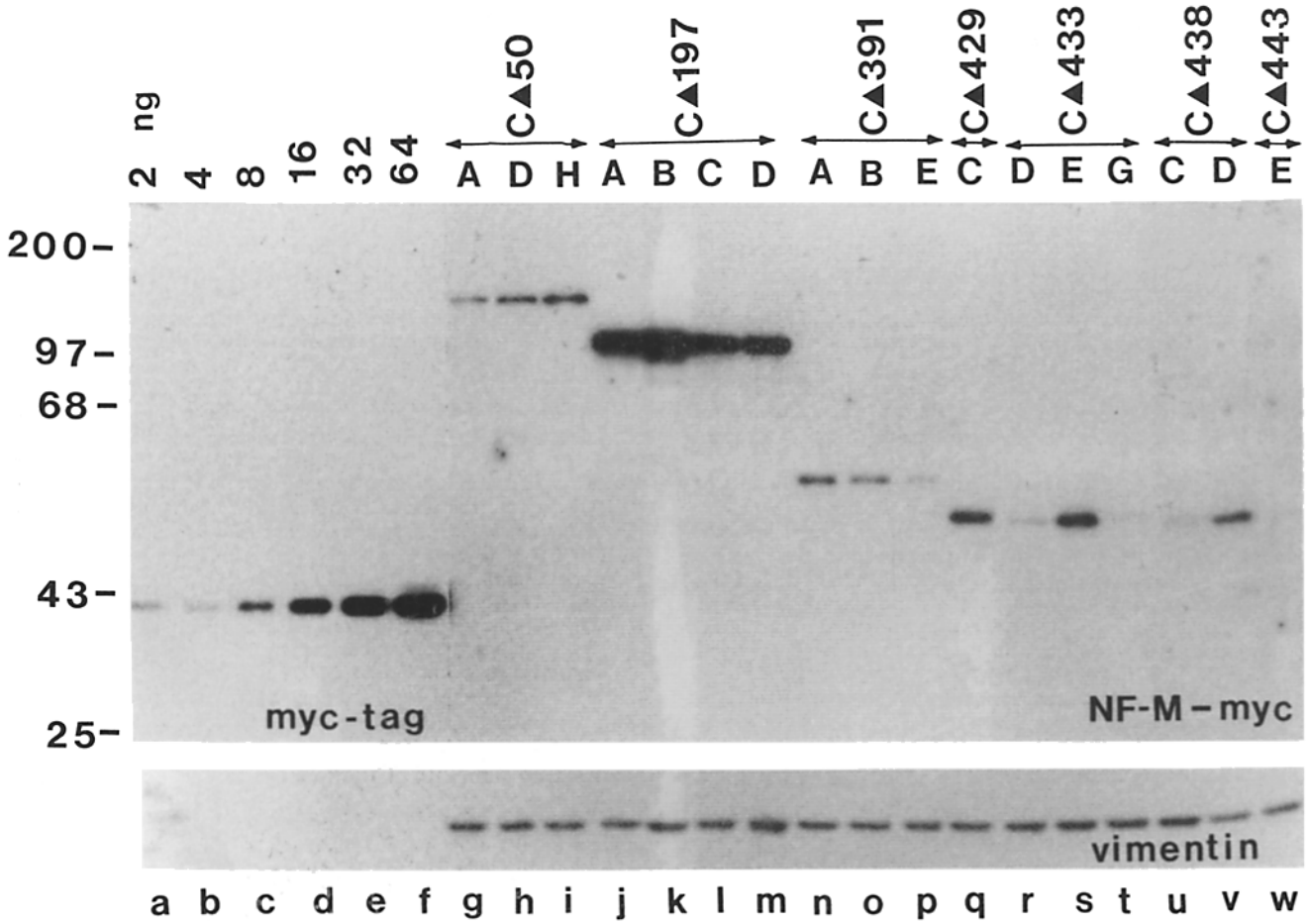

Figure 5. Accumulation of mutant NF-M polypeptides in cell lines stably transfected with pNFM-CΔ*x*. Total cell extracts from cells stably transfected with genes encoding tagged NF-M subunits truncated at their carboxy termini were immunoblotted (20 μg/lane) using the myc-tag monoclonal antibody to quantify the accumulation levels. A series of twofold dilutions of a bacterial extract containing a known amount of a *trp*E/myc fusion protein (shown in nanograms) were immunoblotted in parallel (lanes *a–f*). Similar extracts from mouse L cells stably transfected with pNFM-CΔ50 (lanes *g–i*), pNFM-CΔ197 (lanes *j–m*), pNFM-CΔ391 (lanes *n–p*), pNFM-CΔ429 (lane *q*), pNFM-CΔ433 (lanes *r–t*), pNFM-CΔ438 (lanes *u* and *v*), and pNFM-CΔ443 (lane *w*) were also immunoblotted. The same blot was probed for vimentin using a goat polyclonal vimentin antibody as shown in the bottom panel. For the top panel molecular mass markers in kilodaltons are indicated at the left.

generating a set of standards using parallel immunoblotting with known amounts of a bacterial fusion protein carrying a carboxy-terminal myc tag and a similar set of standards for vimentin, we determined that the average ratio of mutant NF-M polypeptide to endogenous vimentin in the 20% of cells successfully transfected ranged from ≈1:3 (for pNFM-CΔ197) to ≈1:20 (for pNFM-CΔ433).

NF-M Mutants Missing Up to 90% of the Nonhelical Carboxy-tail Domain Incorporate Readily into the Vimentin Network of L Cells

To determine whether the deletion of a portion of the 438 amino acid nonhelical carboxy-terminal tail domain of NF-M would interfere with its ability to assemble into a vimentin filament network, L cells were transiently transfected with the gene constructs shown in Fig. 3 (i.e., pNFM-CΔ50 [deleted 50 amino acids] through pNFM-CΔ443 [deleted 443 amino acids]). Transfected cells were examined by indirect immunofluorescence using the monoclonal antibody against the myc tag to visualize the presence of NF-M derivatives and a polyclonal antibody against vimentin to detect the endogenous vimentin network. As shown in Fig. 4, *A* and *B*, the product of pNFM-CΔ50 was invariably colocalized with the endogenous vimentin network of L cells. Thus, neither

Figure 6. Low levels of the NF-M polypeptides deleted into the carboxy-terminal helical domain disrupt the vimentin network when expressed constitutively. Stably transfected cell lines (*A* and *B*) NFM-CΔ50F, (*C* and *D*)NFM-Δ433D, (*E* and *F*) NFM-CΔ438D, and (*G* and *H*) pNFM-CΔ443E were examined by double-label immunofluorescence. (*A*, *C*, *E*, and *G*) Cells were stained with the Mycl-9E10 monoclonal antibody (which identifies the tagged NF-M subunits) followed by fluorescein-conjugated rabbit anti-mouse IgG and (*B*, *D*, *F*, and *H*) a goat polyclonal vimentin antibody to detect the endogenous vimentin network, followed by rhodamine-conjugated rabbit anti-goat IgG. Bar, 10 μm.

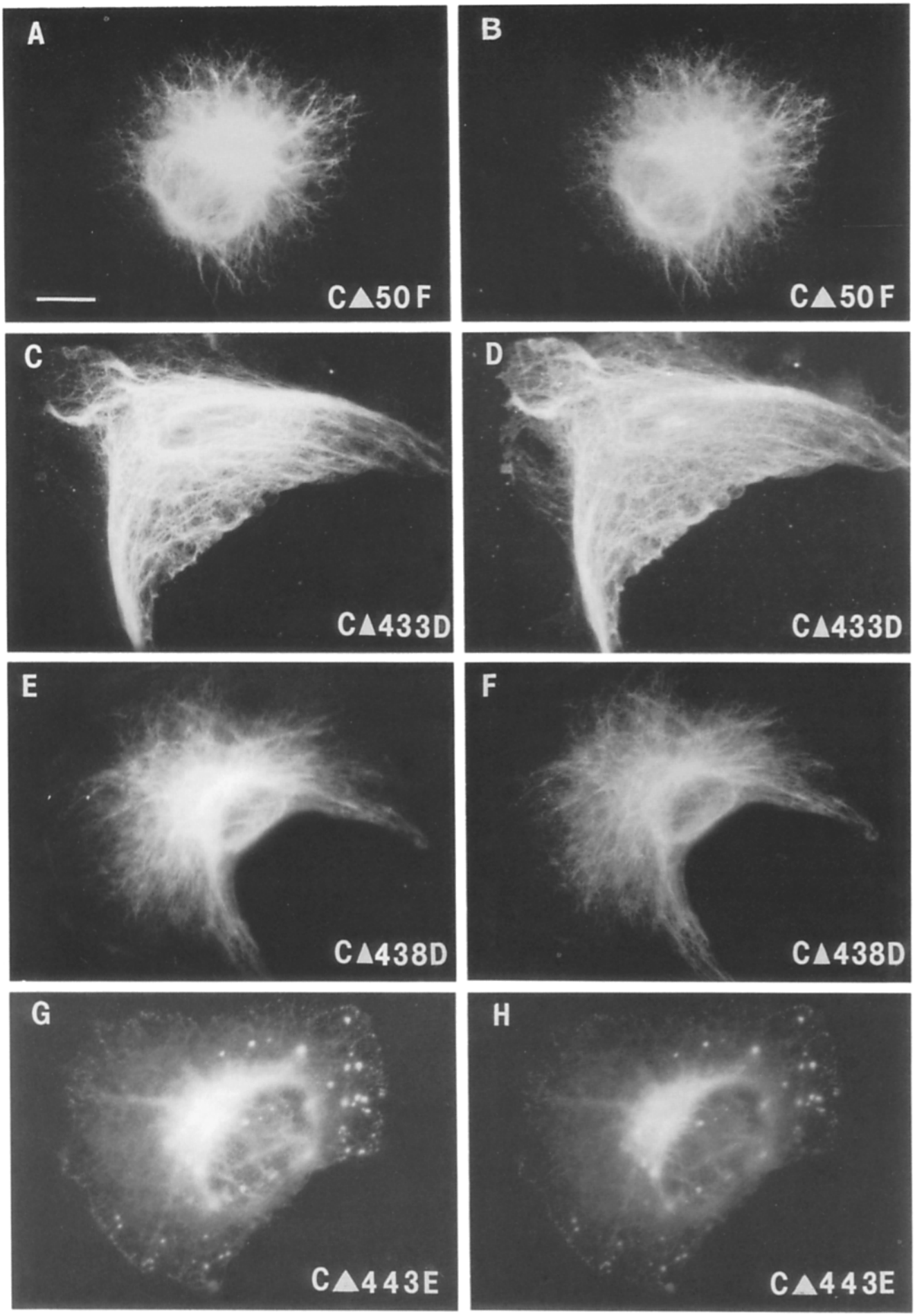
A
C▲50F
B
C▲50F
C
C▲433D
D
C▲433D
E
C▲438D
F
C▲438D
G
C▲443E
H
C▲443E

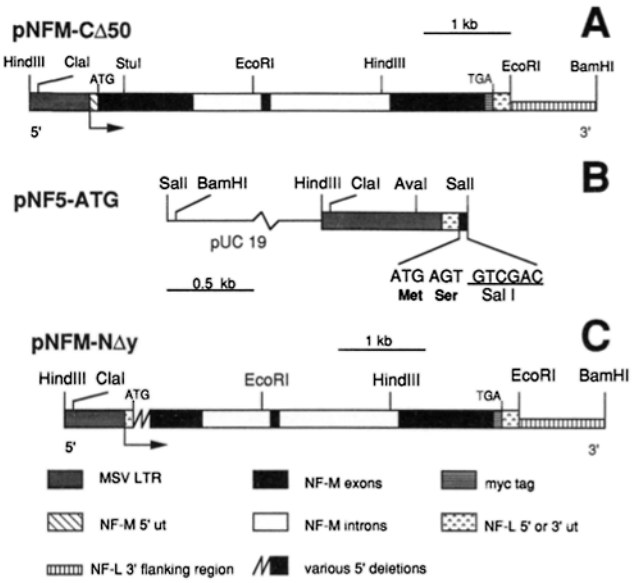

Figure 7. Schematic representations of the components of pNFM-NΔy. (*A*) Schematic diagram of plasmid, pNFM-CΔ50 that was used for generating the set of amino-terminal deletions constructs. (*B*) Schematic diagram of pNF5-ATG which contains the MSV promoter segment fused to the 5′ untranslated region of the mouse NF-L gene, followed by the NF-L translation initiation codon and codon 2 (serine, AGT). (*C*) Schematic drawing of pNFM-NΔy, the set of amino-terminal deletion constructs.

the presence of the tag nor the loss of carboxy-terminal sequences altered the competence of NF-M polypeptides to incorporate into vimentin arrays. Even NF-M molecules missing as many as 391 residues (~90% of the nonhelical carboxy-tail domain) also assembled into the vimentin array without any detectable affect upon cytoskeletal morphology (Fig. 4, *C* and *D*). Thus, the carboxy-tail domain of NF-M is largely dispensable for proper coassembly into an array of filaments that, at least by light microscopy, appears normal.

Mutations Near to or Within the Carboxy-terminal Rod Domain Are IF Array-disrupting Dominant Mutants

In contrast to the normal pattern of assembly observed after expression of mutants retaining >10% of the 438 amino acid nonhelical carboxy-terminal tail domain, a mutant retaining only 9 amino acids of the tail (pNFM-CΔ429) yielded two distinct phenotypes. In 80% of the cells, the tagged NF-M subunits were coaligned with what was an apparently normal vimentin array (e.g., the cell at the left in Fig. 4 *E*); however, in the remaining 20%, mutant NF-M both failed to assemble with vimentin and caused a dramatic reorganization of the vimentin network, a phenotype never seen with mutants carrying substantially larger portions of the tail. For example, as illustrated in the cell to the right in Fig. 4, *E* and *F*, the mutant NF-M was colocalized with vimentin into a series of punctate, cytoplasmic aggregates and a collapsed perinuclear mass of disrupted vimentin filaments. Since the cells in which IF assembly was disrupted were among the most intensely stained with the myc antibody, we interpret this to mean that when expressed at sufficient levels truncated NF-M polypeptides are IF array-disrupting dominant subunits.

The situation for mutants deleted four or five amino acids into the α-helical rod domain (e.g., constructs pNFM-CΔ442 [not shown] or pNFM-CΔ443 [Fig. 4, *G* and *H*]) was even more striking: in >70% of the transfected cells truncated NF-M caused a complete disruption of vimentin filaments, while the remainder showed partial disruption. No myc positive cells displayed a wild-type vimentin array.

We conclude that most, but not all, of the 438 amino acid carboxy-terminal tail is dispensable for assembly of NF-M into IF arrays constructed primarily of wild-type vimentin subunits. Further deletion to include amino acids within the rod domain yields array-disrupting mutants.

Even Low Levels of NF-M Polypeptides Missing Four or Five Residues of the α-Helical Rod Domain Disrupt Vimentin Filament Arrays

To quantify accurately the ratio of mutant NF-M required to disrupt endogenous vimentin arrays and to document whether assembly disruption would be deleterious to cell viability, cell lines were generated that constitutively expressed truncated NF-M subunits. After cotransfection with the neomycin gene, colonies of G418-resistent L cells were selected and individual lines cloned. Fig. 5 shows an immunoblot of twofold serial dilutions of a bacterial extract containing a known amount of a *trpE-myc* fusion protein (lanes *a–f*) and extracts from various stable cell lines (lanes *g–w*) using the monoclonal antibody that recognizes the myc tag. A wide range of levels of NF-M mutant expression was observed: when quantified with the myc fusion protein standards, it was estimated that NF-M levels vary from 1.2 to 0.02% of total cellular protein in the various lines. A similar method has previously been used to show that vimentin constitutes ~2% of total cellular protein in the parental cell line (Monteiro and Cleveland, 1989), a level not significantly changed in any NF-M expressing line (see bottom portions of Fig. 5).

Each cell line stably expressing a mutant NF-M was examined by double indirect immunofluorescence for both mutant NF-M polypeptides and endogenous vimentin. Deletion of a portion (pNFM-CΔ50 to pNFM-CΔ433) or the entirety of the carboxy-terminal tail (pNFM-CΔ438) yielded mutant NF-M polypeptides that integrated normally into the vimentin filament network (as shown in Fig. 6 for pNFM-CΔ50F [*A* and *B*], pNFM-CΔ433D [*C* and *D*] and pNFM-CΔ438E [*E* and *F*]. This was invariably the case even in those lines with the highest levels of mutant NF-M accumulation (lines CΔ197B, CΔ433E, CΔ438D). These results differ from those using the transient transfection in that in all lines expressing mutants retaining an intact rod but deleted in >90% of the tail (e.g., CΔ429 through CΔ438) coassembled with vimentin without obvious disruption. However, this is almost certainly the result of the relative levels of NF-M/vimentin. Quantitative immunoblotting revealed that the highest expressed mutant NF-M in these lines accumulated to the same 5% of vimentin (line 433E) that was seen as the average stoichiometry obtained during transient transfection. Presumably, the 20% of transiently expressing cells that yielded disruption of IF arrays contained levels of mutant NF-M above this threshold.

In contrast, mutations in which the entire carboxy-tail domain and four or five residues of the α-helical rod domain

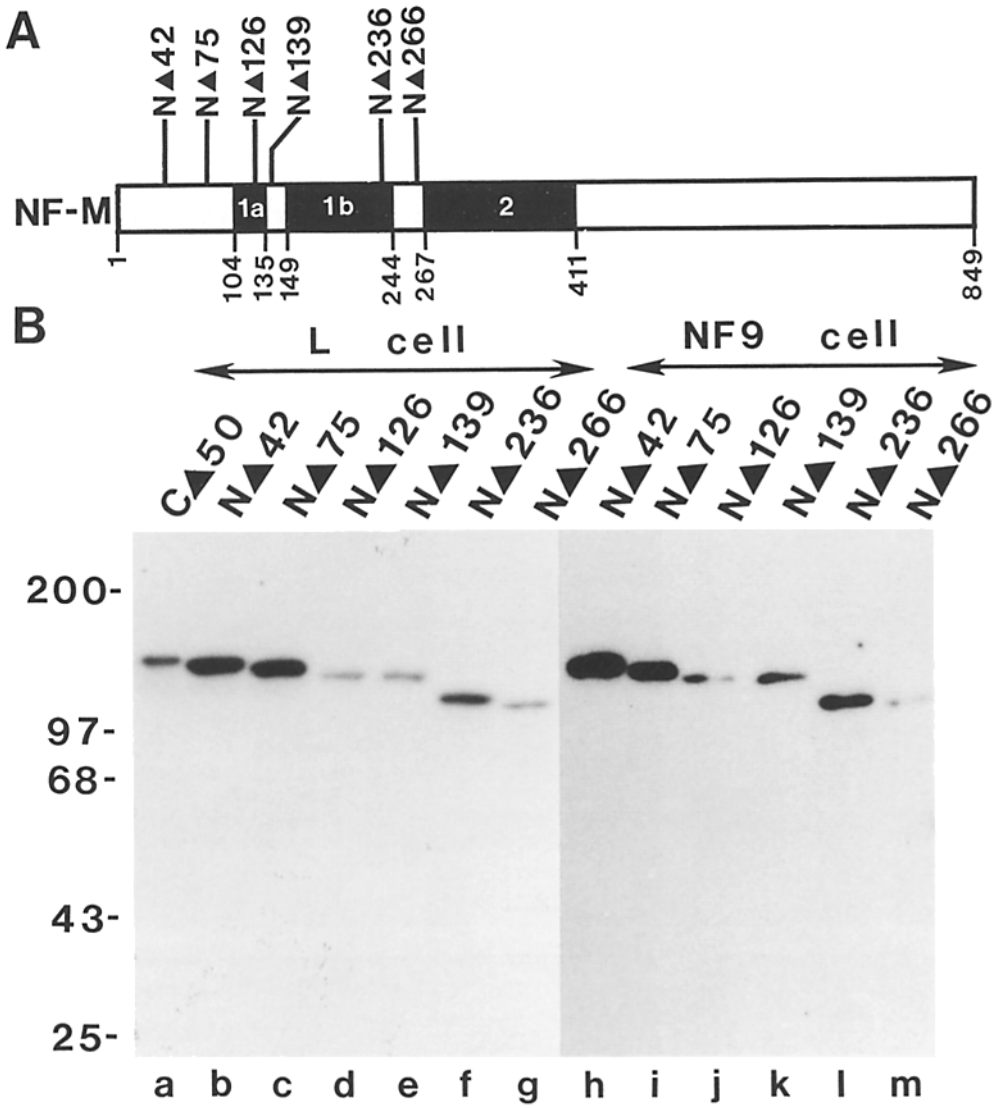

Figure 8. Immunoblot detection of amino-terminal mutant polypeptides after transfection of NFM-NΔ*y* constructs into either mouse L cells or MSV-NF9 cells. (*A*) Schematic diagram of the NF-M polypeptide. The helical domains are represented by the filled rectangles. The deletion endpoint of each mutant is indicated at the top. (*B*) Cells transfected with plasmid DNAs were lysed 40 h after transfection and total cellular proteins were resolved by SDS-PAGE. NF-M mutant polypeptides were detected by immunoblotting using the Mycl-9E10 monoclonal antibody. (Lane *a*) Protein extract from L cells transfected with pNFM-NΔ50 DNA, and (lanes *b–g*) the respective pNFM-CΔ*y* DNAs. (Lanes *h–m*) Protein extracts from MSV-NF9 cells transfected with the respective pNFM-NΔ*y* DNAs. Molecular mass markers in kilodaltons are indicated at the left.

were deleted yielded lines in which the assembly of the endogenous vimentin network was partially disrupted (illustrated for NFM-CΔ443E in Fig. 5, *G* and *H*). For these mutants, most NF-M was colocalized with vimentin into punctate aggregates scattered throughout the cytoplasm, although some filamentous staining juxtaposed to the nucleus was also apparent both for vimentin and for the mutant NF-M. This disruption (albeit incomplete) of the normal vimentin array was seen even when the mutant polypeptide (NFM-CΔ443) was only 0.02% of total cellular protein (line CΔ443E), while the vimentin content was 2%. Therefore, as little as 1 part in 100 of this mutant polypeptide (deleted only five amino acids into the rod domain) is sufficient to disrupt assembly of a portion of the vimentin network of L cells. Further, examination of the growth rate of the mutant cells revealed no differences relative to the parental cells with intact arrays, demonstrating that the partial disruption of the IF array did not affect mitotic growth.

Construction and Expression of Amino-terminal Deletions of NF-M

We also generated a set of amino-terminal deletions beginning with the construct pNFM-CΔ50 already tagged with c-*myc* at its carboxy terminus. From this, we used exonuclease III to generate a series of amino-terminal deletions into the NF-M coding region. To provide an appropriate translation initiation site, the 5′ untranslated region together with the first two codons of NF-L were added (see Fig. 7 and Materials and Methods). DNA sequencing was used to identify deletions in which the ATG was linked to the correct reading frame of NF-M. The mutant constructs (Fig. 8 *A*) are denoted by pNFM-NΔ*y*, where *y* refers to the number of amino acids removed from the amino-terminal domain of NF-M (the precise end point of each deletion is marked in Fig. 1).

Each construct was transfected into mouse fibroblasts and

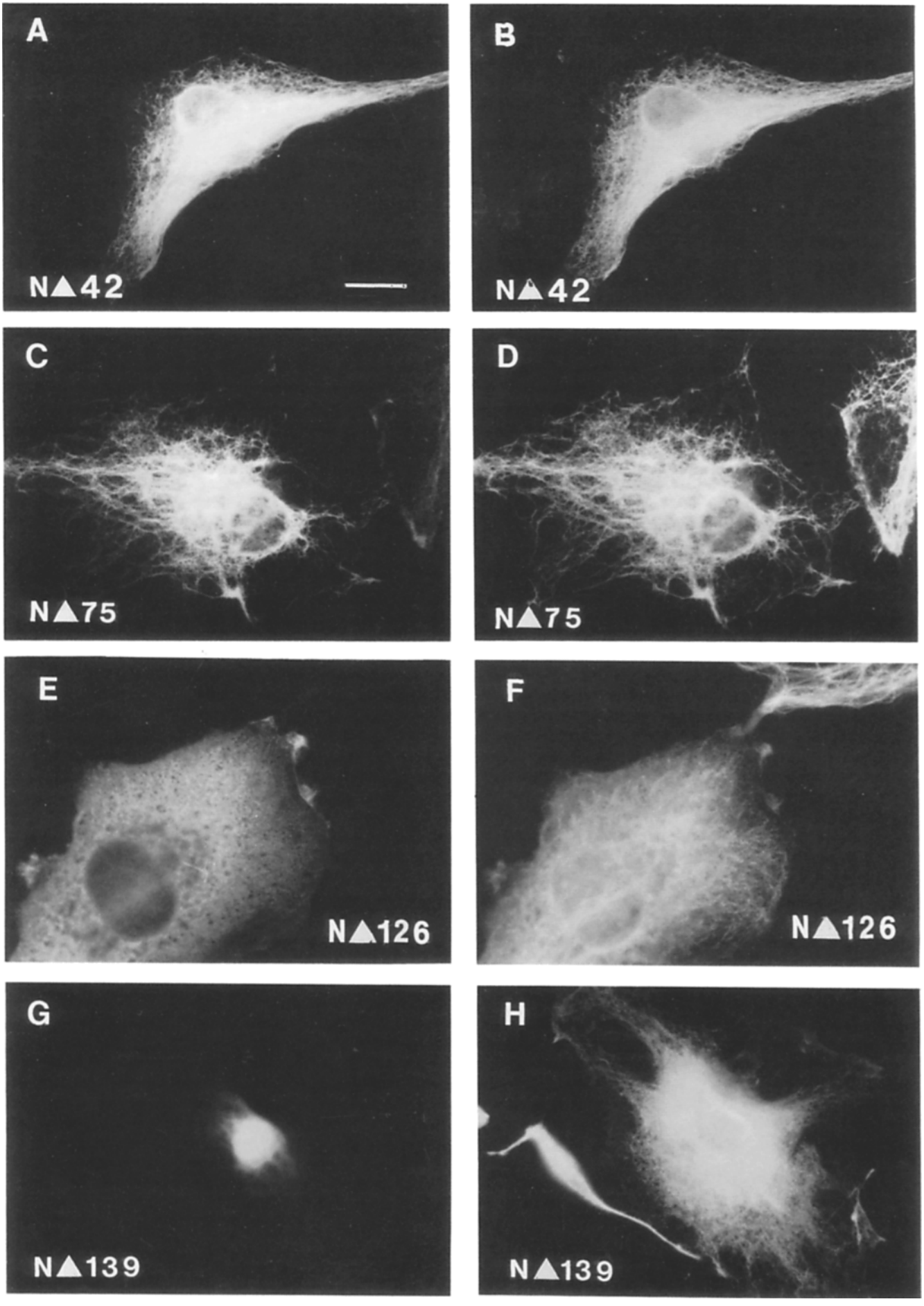
A
NΔ42
B
NΔ42
C
NΔ75
D
NΔ75
E
NΔ126
F
NΔ126
G
NΔ139
H
NΔ139

total cellular proteins were analyzed 40-h posttransfection. Protein samples were resolved by SDS-PAGE and immunoblotted with the monoclonal antibody against the myc tag. As shown in Fig. 8 *B* (lanes *b–g*), a single immunoreactive polypeptide was detected in each transfected cell extract. In all cases, the size was consistent with that predicted from the sequence data. By using parallel immunoblotting of known molar amounts of myc-bearing fusion proteins combined with immunofluorescence that revealed ~20% of the cells were successfully transfected, we calculate that in transfected cells the molar ratio of mutant polypeptide to endogenous vimentin ranged from ~1:2 (for mutant pNFM-NΔ42) to ~1:50 (for mutant pNFM-NΔ139).

NF-M Truncated in Up to 70% of 103 Amino Acid Head Domain Retains Coassembly Competence

To test whether the removal of portions of the nonhelical amino-head domain yields an assembly-competent NF-M subunit, L-cells were transiently transfected with constructs pNFM-NΔ42 and pNFM-NΔ75 and examined by indirect immunofluorescence. As before, a monoclonal antibody against the myc tag was used to visualize the presence of NF-M mutant polypeptides, while a polyclonal antibody against vimentin was used to detect the vimentin array. As shown in Fig. 9, *A* and *B*, the NF-M polypeptide truncated in the amino-terminal 42 residues (NFM-NΔ42) was incorporated into a fine filamentous array that completely colocalized with the endogenous vimentin network. Further truncation of the first 75 amino acids yielded a subunit that also continued to colocalize with vimentin (Fig. 9, *C* and *D*). However, while the vimentin array was like that in untransfected cells, in most transfected cells the NF-M subunits were more prominently localized to the perinuclear region with only weak staining appearing at the most peripheral portions of the cytoplasm. Therefore, while perhaps not completely wild type, it is clear that NF-M molecules missing up to 70% of the nonhelical amino-head domain retain substantial competency for assembly into IF networks, at least in the presence of wild-type vimentin polypeptides.

Semirecessive Amino-Terminal Mutants Identify a Determinant Necessary for Efficient Assembly into IF Arrays

We also transfected mutant constructs deleted into the rod from the amino terminus (e.g., pNFM-NΔ126 to pNFM-NΔ266; Fig. 8). A mutant polypeptide deleted 23 amino acids into the rod domain (pNFM-NΔ126) was assembly incompetent as reflected by the diffuse cytoplasmic staining pattern (Fig. 9 *E*), a pattern seen in all transfected cells. In contrast with the dominant carboxy-terminal rod mutants, the presence of this mutant polypeptide did not lead to complete collapse of the endogenous vimentin array in any of the transfected cells (Fig. 9 *F*) even though quantitative immunoblotting revealed that its average abundance relative to vimentin (1:50) was similar to disruptive carboxy-terminal mutants. Instead, the vimentin remained filamentous but the arrays appeared comprised of many fine filaments. Deletion of an additional 13 amino acids to remove the entirety of helix 1a (pNFM-NΔ139) yielded a subunit that localized to perinuclear aggregates (Fig. 9 *G*). Although its average level was again 1/50th the level of vimentin, the vimentin network was only partially fragmented, appearing as a fine meshwork of apparently shorter, cytoplasmic filaments (Fig. 9 *H*). Clearly, these amino-terminal rod mutations yield subunits that for the most part fail to interact (i.e., localize) with wild-type IF subunits. Vimentin remains assembled into filaments, but the mutants fragment the normal IF array into a finer filamentous network. Further deletions into the rod (pNFM-NΔ236 and pNFM-NΔ266) yielded no detectable immunofluorescence signals in cytoskeleton preparations. Since the mutant polypeptides were detected by immunoblotting (Fig. 8, lanes *f* and *g*), we conclude that these polypeptides are incompetent for assembly into filaments and are soluble. Since none of the amino-terminal rod deletions we examined colocalized with or disrupted assembly of vimentin into filaments, we conclude that sequences within the region spanning residues 75–126 of NF-M are necessary for its efficient interaction with vimentin to form dimers and/or other oligomers.

Mutations of NF-M Near the Carboxy-Terminal Rod Domain Disrupt NF-L Arrays

Since it was possible that the domains of NF-M required for coassembly with vimentin differ from those necessary for assembly with its normal partner NF-L, we also examined the consequences of expression of mutant NF-M subunits in a cell line (MSV-NF9; Monteiro and Cleveland [1989]) that stably accumulates NF-L to high levels (~8% of cell protein). Various carboxy-terminal deletion constructs were transiently transfected into MSV-NF9 cells and protein extracts immunoblotted. Polypeptides of the expected molecular masses (shown in Fig. 3 *B*, lanes *k–q*) were observed. As before, indirect immunofluorescence with a monoclonal antibody against the myc tag was used to stain for the presence of NF-M polypeptides while a polyclonal antibody against NF-L was used to stain the endogenous NF-L array. As shown in Fig. 10 *A* and *B*, the polypeptide encoded by pNFM-CΔ197 (as well as pNFM-CΔ50 and pNFM-CΔ391; not shown) was coassembled into the NF-L array. Thus, NF-M mutant polypeptides missing up to 90% of their carboxy-tail domain assembled properly into the NF-L array. In contrast, mutants deleted closer to the carboxy-terminal rod domain were dominant disruptors of NF-L arrays in 50% of the transfected cells. For example, as shown by the cell in the center of Fig. 10, *C* and *D*, transfection of pNFM-CΔ438 (deleted in the entire tail) yielded punctate staining containing NF-M and wild-type NF-L throughout the cytoplasm, as well as large perinuclear aggregates. This disruption of NF-L

Figure 9. Assembly properties of NF-M subunits missing portions or the entirety of the nonhelical amino-head domain. Mouse L cells grown on coverslips were transfected with (*A* and *B*) plasmids pNFM-NΔ42, (*C* and *D*) pNFM-NΔ75, (*E* and *F*) pNFM-NΔ126, and (*G* and *H*) pNFM-NΔ139. Cells were stained 40 h after transfection as described in Fig. 4 for (*A*, *C*, *E*, and *G*) NF-M subunits and (*B*, *D*, *F*, and *H*) endogenous vimentin. Bar, 10 μm.

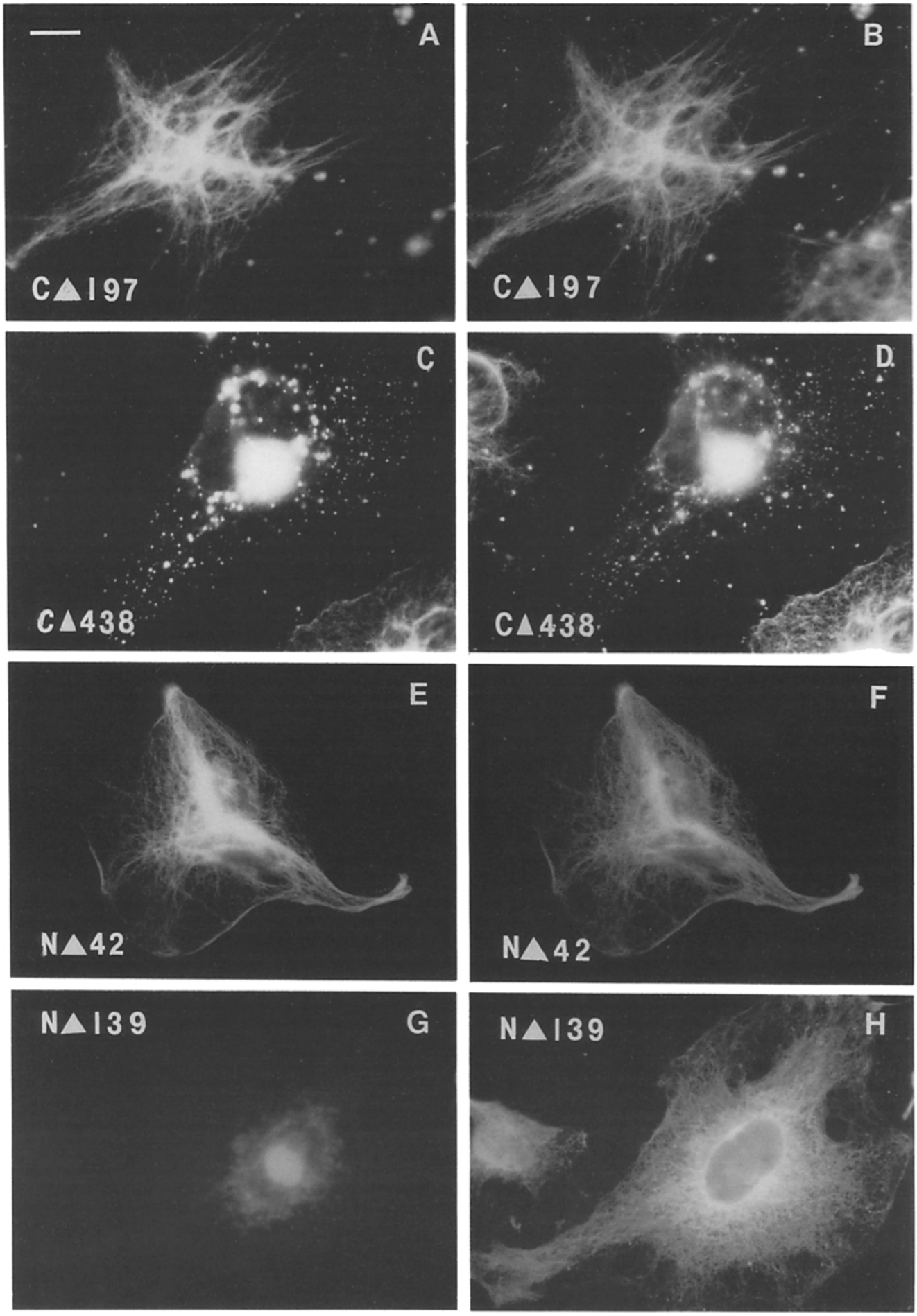
A
C▲197
B
C▲197
C
C▲438
D
C▲438
E
N▲42
F
N▲42
N▲139
G
N▲139
H

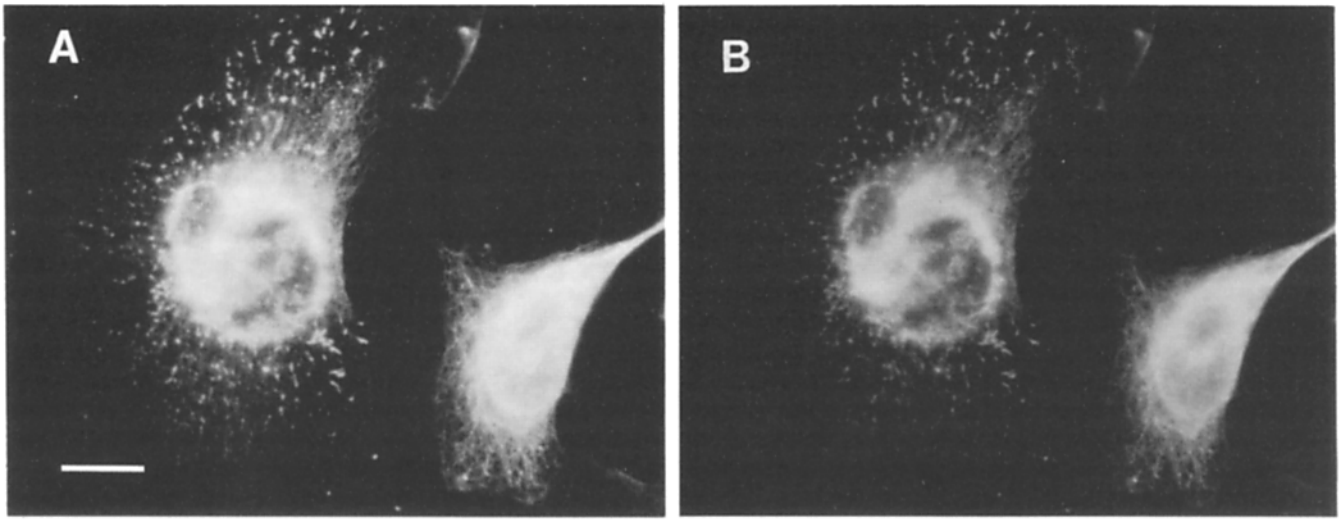

Figure 11. NF-M molecules missing 70% of the amino-head and 90% of the carboxy-tail domains are assembly-disrupting dominant mutants. Mouse L cells grown on coverslips were transfected with plasmid pNFM-NΔ75/CΔ931. (*A*) The mutant NF-M polypeptides were detected 40 h posttransfection using Mycl-9E10 monoclonal antibody followed by fluorescein-conjugated rabbit anti-mouse IgG and (*B*) vimentin was visualized in the same transfected cells with a goat polyclonal vimentin antibody followed by a rhodamine-conjugated rabbit anti-goat IgG. Bar, 10 μm.

arrays was seen as early as 19-h posttransfection and occurred at average NF-M/NF-L stoichiometries of 1:20. Some NFM-CΔ438 expressing cells showed more normal IF arrays (e.g., the cell at the lower right in Fig. 10, *C* and *D*).

NF-M Subunits Truncated into the Amino-terminal Rod Domain Do Not Disrupt NF-L Arrays

When amino-terminal NF-M deletion constructs were transfected into NF-L expressing MSV-NF9 cells, each construct directed the synthesis of the predicted NF-M mutant polypeptide (revealed by immunoblot; Fig. 8 *B*, lanes *h–m*). Indirect immunofluorescence examination of the transfected cells again showed that mutant polypeptides missing up to 70% of their amino-head domain remained assembly competent. Mutant polypeptides missing 42 amino-terminal residues (NFM-NΔ42; Fig. 10, *E* and *F*) or 75 residues (NFM-NΔ75; not shown) incorporated properly into the endogenous NF-L array. However, mutations that extended into the rod domain were not assembly competent and the mutant polypeptides formed a large aggregate adjacent to the nucleus (such as NFM-NΔ139; Fig. 10 *G*). The corresponding endogenous NF-L array still retained a network of NF-L-containing filaments (Fig. 10 *H*), although as in the case of vimentin-expressing cells (Fig. 9 *H*) the IF array appeared fragmented into a meshwork of finer filaments. While this suggests that such mutants result in a minor disruption in NF-L arrays (at a NF-M/NF-L ratio of 1:25 as revealed by quantitative immunoblotting), it is clear that efficient association of NF-M into NF-L dimers, oligomers, and/or filaments requires some residues in the amino-terminal domain between 75 and 126.

Identifying the Minimal NF-M Domain That Is Assembly Competent

Having determined that subunits truncated to leave at least 28 amino acids of the head (NFM-NΔ75) or 47 amino acids of the tail (NFM-CΔ391) retained full coassembly competence, we next tested whether NF-M truncated to these amino- and carboxy-terminal borders defined the minimal assembly competent domain. A gene missing 75 residues of the amino- and 391 residues of the carboxy-terminal domain (NFM-NΔ75/CΔ391) was prepared. Transfection of this nearly headless and tailless NF-M gene revealed two phenotypes. In 30% of the transfected cells the mutant NF-M subunits were assembly competent and coaligned with the vimentin array (e.g., the cell at the right in Fig. 11, *A* and *B*). However, in the majority of the transfected cells, the mutant NF-M produced a dominant phenotype that was reminiscent of the carboxy-terminal assembly-disrupting mutants. As shown by the cell at the left in Fig. 11, *A* and *B*, the mutant polypeptide was colocalized with vimentin into a disrupted array that contained punctate cytoplasmic aggregates and a collapsed perinuclear mass. Similar results were obtained when the same gene was transfected into NF-L expressing MSV-NF9 cells (not shown). Even after restoring an additional 33 amino-terminal residues (NFM-NΔ42/CΔ391) we observed disruption in ~70% of transfected cells. Since neither deletion of the amino-terminal 75 residues or as many

Figure 10. Expression of mutant NF-M polypeptides in fibroblasts that stably express high levels of NF-L. MSV-NF9 cells grown on coverslips were transiently transfected with (*A* and *B*) pNFM-CΔ197, (*C* and *D*) pNFM-CΔ438, (*E* and *F*) pNFM-NΔ42, or (*G* and *H*) pNFM-NΔ139. Cells were stained 40 h after transfection with the Mycl-9E10 monoclonal antibody followed by fluorescein-conjugated rabbit anti-mouse IgG to visualize the NF-M mutant polypeptides and a rabbit polyclonal NF-L antibody followed by rhodamine-conjugated goat anti-rabbit IgG to detect the endogenous NF-L array. (*A*, *C*, *E*, and *G*) NF-M staining; (*B*, *D*, *F*, and *H*) NF-L staining. Bar, 10 μm.

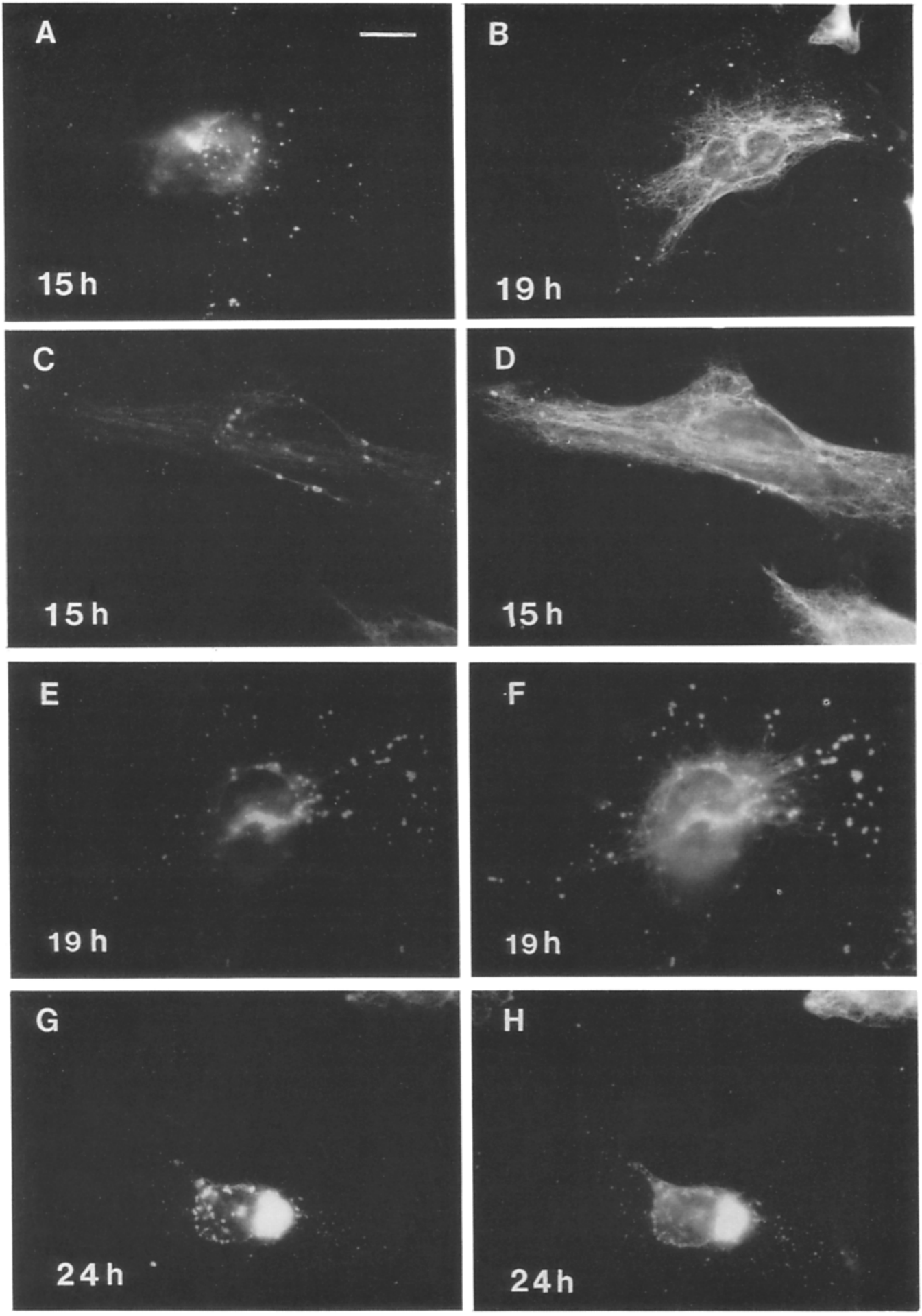
A
15 h
B
19 h
C
15 h
D
15 h
E
19 h
F
19 h
G
24 h
H
24 h

as 391 carboxy-terminal residues alone was disruptive (Figs. 4 *C* and 9 *C*), these findings demonstrate that the nonhelical domains do play some role in assembly of NF-M into IF arrays.

Disruption of Vimentin Arrays Occurs with a Half-Time of Less Than 3 h

To examine the rapidity with which an endogenous wild-type IF array could be disrupted by expression of a mutant subunit, we followed the accumulation of an assembly disrupting dominant mutant (deleted five amino acids into the carboxy-terminal rod domain) after transient transfection. The earliest time at which mutant protein was detectable by immmunofluorescence was 15-h posttransfection (Fig. 12, *A* and *C*). These newly accumulated mutants localized to a series of dispersed cytoplasmic aggregates (which contained too little protein to be quantified by immunoblot) that also contained wild-type vimentin (Fig. 12 *D*). These aggregates had little effect on the overall vimentin array which remained nearly fully assembled (Fig. 12 *D*). However, in a subsequent 4-h period, a level of mutant polypeptide accumulated to yield an average content in transfected cells of 1:200 for NF-M/vimentin and immunofluorescence demonstrated that this was accompanied by partial disruption of the endogenous IF array (Fig. 12, *B* and *F*). In most cells expressing this mutant, complete disruption of the endogenous array (Fig. 12, *G* and *H*) was seen 24-h posttransfection (9 h after the mutant protein was first observed), when the average proportion of mutant to vimentin had risen to 1:50. The essentially complete disruption of the endogenous filament array within a 9-h period indicates that in the presence of mutant subunits, collapse or disassembly of the array must occur with a half time of 3 h or less.

Discussion

The use of DNA transfection to force coexpression of truncated NF-M subunits with either wild-type vimentin or NF-L polypeptides has allowed us an initial examination of the domains essential for in vivo assembly of this neurofilament subunit. As might have been anticipated, no mutation from either the amino or carboxy terminus that truncates into the predicted helical domain yields an assembly competent subunit; rather, in addition to the 310 amino acid rod, the minimal NF-M domain that we have shown to coassemble includes 26 amino acids of the head. While at the carboxy terminus deletions that precisely remove the entire tail (e.g., NFM-CΔ438) can be assembled, this conclusion is misleading since this NF-M mutant (as well as one with nine additional amino acids of the tail) become array-disrupting dominant mutants when expressed at higher ratios to wild-type subunits (Fig. 10, *C* and *D*). While in vitro assembly experiments with these or similar mutant polypeptides will be required to establish definitively the precise assembly products of wild-type and mutant polypeptides (and at various stoichiometries), our stable transfectants that express NF-M subunits truncated into the NF-M rod yield an unambiguous in vivo finding: mutations in this domain are invariably assembly-disrupting mutants even when accumulated to levels only 1% of the wild-type subunit.

The minimal NF-M subunit that retains assembly competence (but only when present in low molar amounts) contained 30 amino acids of head and 47 amino acids of tail domain, respectively, in addition to the complete helical segment. That the rod domain is largely sufficient for assembly is consistent with preceding analyses of other intermediate filament subunits. By using a transfection protocol after which we modeled our experiments, Albers and Fuchs (1987, 1989) documented that a minimal domain of the type I human keratin K14 required for coassembly with a wild-type type II keratin was limited to the rod domain preceded by an eight amino acid head. Dispensability of at least one of the two tails in the keratin heterodimer of one type I and one type II chain was also emphasized in a more natural context by discovery of a bovine keratin (K19) that is nearly tailless (Bader et al., 1986). However, the conclusion that the rod domain alone is sufficient for assembly of an IF network may be misleading, since it is not known whether a tailless pair of type I and II keratins can assemble. We have shown here that the rod elements of NF-M (and in the companion paper of NF-L; Gill et al., 1990) cannot support filament network assembly without assistance from wild-type subunits. Whether rod elements alone can support assembly of the type III IF subunits is not yet tested. Neither is the case clear at present for nuclear lamins since truncation of the lamin A tail results in aberrant cytoplasmic assembly due (at least in part) to deletion of the nuclear localization signal carried within the tail domain (Loewinger and McKeon, 1988).

Further distinctions from the previous work with keratins are the effects of amino-terminal truncations. Deletions into the helical domain from either the carboxy or amino terminus of type I human keratin K14 yield mutant subunits that disrupt networks of wild-type type I and II keratins (Albers and Fuchs, 1987, 1989). Moreover, the amino-terminal mutations are sufficiently severe that cells expressing them do not recover from transient expression (Albers and Fuchs, 1989). In contrast, for NF-M (and NF-L; Gill et al., 1990) the amino-terminal deletions, while assembly incompetent, are at least partially recessive and affect the wild-type filament array much less markedly than do the carboxy-terminal mutants. We infer that this "pseudo" recessive nature reflects the deletion of a domain(s) (within amino acids 76–126 of NF-M) that is necessary for efficient interaction with normal subunits. Of course, we do not put too fine a point on it since in vitro reassembly reactions are required to document this more directly.

Indeed, despite the strength of such transfection experiments in their ability to track the overall IF network, this approach also brings an inherent weakness: the limited resolu-

Figure 12. Kinetics of endogenous IF disruption during accumulation of an assembly-disrupting NF-M mutant (NFM-CΔ443). L cells grown on coverslips were transiently transfected with pNFM-CΔ443. Cells were stained (*A*, *C*, and *D*) 15, (*B*, *E*, and *F*) 19, or (*G* and *H*) 24-h post-transfection. NFM-CΔ443 polypeptides or vimentin were visualized as described in earlier figures. (*A*, *C*, *E*, and *G*) NFM-CΔ443 staining; (*B*, *D*, *F*, and *H*) vimentin staining. *C* and *D*, *E* and *F*, and *G* and *H* are pairs of double immunofluorescent images visualizing NFM-CΔ443 and vimentin. *A* and *B* are images of cells stained only for (*A*) NFM-CΔ443, or (*B*) vimentin. Bar, 10 μm.

tion cannot determine precisely where assembly is blocked (at formation of dimers, tetramers, or other oligomers). Indeed, it is possible that some of the mutant polypeptides are assembled into bona fide filaments, but that incorporation of the mutants disrupts competence for other interactions needed for assembly or maintenance of extended IF arrays. Electron microscopic analysis as well as the in vitro assembly experiments mentioned above are needed to address more clearly the underlying structure(s) of the aggregates formed.

Another caution that tempers interpretation of mutagenesis experiments is that the failure of a mutant (either point or deletion) to share a property of the wild-type protein (e.g., assembly competence) may not be due to mutation within a domain required for that property. Rather, it may result from mutagenesis-induced changes in protein conformation in a remaining (most often adjacent) domain. In this regard, the formal possibility remains that some of the assembly disruptive properties of the mutant subunits may derive from the carboxy-terminal myc tag, although given the apparent wild-type assembly of other mutants carrying the same tag, we consider this unlikely.

A final ambiguity that arises from transient expression is the precise level of accumulation. While we have accurately measured the average level of accumulation, we cannot be certain of the level in individual cells. Based on fluorescence intensity, we believe that for those mutants displaying coassembly in some cells, but disrupting arrays in others (e.g., NFM-CΔ438), the differences in phenotype result from differences in the amount of mutant. However, another (not mutually exclusive) explanation is cell cycle–dependent disruption of IF arrays, a clearly interesting possibility, but one not yet addressed by our experiments.

In any event, the relatively rapid disruption of endogenous vimentin (or NF-L) reinforces that IF arrays must be dynamic. This point was unequivocally established for keratins when Albers and Fuchs (1989) showed that mutant keratins initially caused a retraction of the keratin array from the plasma membrane, followed by collapse and disruption of the entire network. For the type III (vimentin) and type IV (NF) arrays analyzed here, we find substantial disruption within a 4-h period during which the mutant NF-M is first accumulated. Even at the time that disruption is complete (~9 h after first appearance of the mutant), we calculate the average level in transfected cells of mutant subunit to be only ~1/50 of the wild type. The disassembly and localization of wild-type subunits into coaggregates with newly made mutant polypeptides is consistent with only two general scenarios (which are not mutually exclusive): either IF filaments have an intrinsic dynamic behavior with a maximal filament half-life of <3 h (such a half life would yield disassembly of ~90% of the initial IF array in 9 h) or subunits freely exchange along the length of existing filaments. In the first possibility, mutant subunits would block reassembly of wild-type proteins liberated by natural or mutant-induced filament disassembly. In the second, incorporation of the mutant subunits along the length could trigger filament fragmentation leading ultimately to disruption of the entire wild-type array. This latter possibility is particularly appealing in view of STEM measurements that have indicated that in vitro reassembled keratin IFs (Steven et al., 1983; Engel et al., 1985) or native NF (Aebi et al., 1988) do not have a constant number of IF subunits per unit length. This is also consistent with the finding that newly synthesized vimentin subunits are apparently incorporated at many sites along the length of existing filaments (Ngai et al., 1990).

The in vivo role of intermediate filaments has been a most troublesome question. Neither the absence nor (as we have now shown) disruption of type III IF arrays affects mitotic growth of cultured cells. Indeed, there is no compelling experimental evidence that establishes an in vivo function of any IF protein. However, for NF, we and our colleagues have identified a strong correlation in mammals between NF content and axonal diameter in large bore, myelinated axons of the peripheral nervous system (Hoffman et al., 1984, 1985, 1987; Hoffman and Cleveland, 1988). The identification of assembly-disrupting dominant mutants, as we have done here, should now allow a direct test of this potential function by analysis of the consequences in transgenic mice of in vivo expression of these mutant NF-M subunits.

We thank Peter Sarger and Hugh Pelham (Medical Research Council, Cambridge, England) for providing the c-*myc* tag and Gerrard Evan (Imperial Cancer Research Fund, London) for the cells producing his monoclonal antibody Myc-9E10.

This work has been supported by grant NS27036 from the National Institutes of Health to D. W. Cleveland. P. C. Wong has been supported in part by a postdoctoral fellowship from the Muscular Dystrophy Association.

Received for publication 13 June 1990 and in revised form 19 July 1990.

Note Added in Proof. X. Lu and E. B. Lane (1990. *Cell.* 62:681–696) have recently reported coexpression of both wild-type and mutant type I and II keratin genes in fibroblast cells that accumulate no endogenous keratin filaments. Similar to our finding that a portion of the head and tail domains are required for assembly of NF-M, they found that keratin filament assembly requires intact amino- and carboxy-terminal domains on at least one of the two subunits.

References

Aebi, U., M. Haner, J. Troncoso, R. Eichner, and A. Engel. 1988. Unifying principles in intermediate filament (IF) structure and assembly. *Protoplasma.* 145:73–81.

Albers, K., and E. Fuchs. 1987. The expression of mutant epidermal keratin cDNAs transfected in simple epithelial and squamous cell carcinoma lines. *J. Cell Biol.* 105:791–806.

Albers, K., and E. Fuchs. 1989. Expression of mutant keratin cDNAs in epithelial cells reveals possible mechanisms for initiation and assembly of intermediate filaments. *J. Cell Biol.* 108:1477–1493.

Bader, B. L., T. M. Magin, M. Hatzfeld, and W. W. Franke. 1986. Amino acid sequence and gene organization of cytokeratin no. 19, an exceptional tail-less intermediate filament protein. *EMBO (Eur. Mol. Biol. Organ.) J.* 5:1865–1875.

Carden, M. J., W. W. Schlaepfer, and V. M.-Y. Lee. 1985. The structure, biochemical properties and immunogenicity of neurofilament peripheral regions are determined by phosphorylation state. *J. Biol. Chem.* 260:9805–9817.

Engel, A., R. Eichner, and U. Aebi. 1985. Polymorphism of reconstituted human epidermal keratin filaments: determination of their masses-per-unit-length and width by scanning transmission electron microscopy (STEM). *J. Ultrastruc. Res.* 90:323–325.

Evan, G. I., G. K. Lewis, G. Ramsay, and J. M. Bishop. 1985. Isolation of monoclonal antibodies specific for human c-myc proto-oncogene product. *Mol. Cell. Biol.* 5:3610–3616.

Fliegner, K. H., G. Y. Ching, and R. K. H. Liem. 1990. The predicted amino acid sequence of α-internexin is that of a novel neuronal intermediate filament protein. *EMBO (Eur. Mol. Biol. Organ.) J.* 9:749–755.

Franke, W. W. 1987. Nuclear lamins and cytoskeletal intermediate filament proteins: a growing multigene family. *Cell.* 48:3–4.

Gardner, E. E., D. Dahl, and A. Bignami. 1984. Formation of 10 nm filaments from the 150kD neurofilament protein in vitro. *J. Neurosci. Res.* 11:145–155.

Geisler, N., and K. Weber. 1981. Self-assembly *in vitro* of the 68,000 molecular weight component of the mammalian neurofilament triplet proteins into intermediate-size filaments. *J. Mol. Biol.* 151:565–571.

Geisler, N., and K. Weber. 1982. The amino acid sequence of chicken muscle desmin provides a common structural model for intermediate filament pro-

teins. *EMBO (Eur. Mol. Biol. Organ.) J.* 1:1649–1656.
Geisler, N., and K. Weber. 1986. Structural aspects of intermediate filaments. *In* Cell and Molecular Biology of the Cytoskeleton. J. W. Shay, editor. Plenum Publishing Corp., New York. 41–68.
Geisler, N., and K. Weber. 1987. Location and sequence characterization of the major phosphorylation sites of the high molecular mass neurofilament proteins M and H. *FEBS (Fed. Eur. Biochem. Soc.) Lett.* 221:403–407.
Geisler, N., S. Kaufmann, S. Fischer, U. Plessmann, and K. Weber. 1983. Neurofilament architecture combines structural principles of intermediate filaments with carboxy-terminal extensions increasing in size between triplet proteins. *EMBO (Eur. Mol. Biol. Organ.) J.* 2:1295–1302.
Geisler, N., S. Fischer, J. Vanderkerchove, U. Plessmann, and K. Weber. 1984. Hybrid character of a large neurofilament protein (NF-M): intermediate filament type sequence followed by a long acidic carboxy-terminal extension. *EMBO (Eur. Mol. Biol. Organ.) J.* 3:2701–2706.
Geisler, N., U. Pressmann, and K. Weber. 1985. The complete amino acid sequence of the major mammalian neurofilament protein (NF-L). *FEBS (Fed. Eur. Biochem. Soc.) Lett.* 182:475–478.
Gill, S. R., P. C. Wong, M. J. Monteiro, and D. W. Cleveland. 1990. Assembly properties of dominant and recessive mutations in the small mouse neurofilament (NF-L) subunit. *J. Cell Biol.* 111:2005–2019.
Hirokawa, N., M. A. Glicksman, and M. B. Willard. 1984. Organization of mammalian neurofilament polypeptides within the neuronal cytoskeleton. *J. Cell Biol.* 98:1523–1536.
Hoffman, P. N., and D. W. Cleveland. 1988. Neurofilament and tubulin expression recapitulates the developmental program during axonal regeneration: Induction of a specific β-tubulin isotype. *Proc. Natl. Acad. Sci. USA.* 85:4530–4533.
Hoffman, P. N., J. W. Griffin, and D. L. Price. 1984. Control of axonal caliber by neurofilament transport. *J. Cell Biol.* 99:705–714.
Hoffman, P. N., G. W. Thompson, J. W. Griffin, and D. L. Price. 1985. Changes in neurofilament transport coincide temporally with alterations in the caliber of axons in regenerating motor fibers. *J. Cell Biol.* 101:1332–1340.
Hoffman, P. N., D. W. Cleveland, J. W. Griffin, P. W. Landes, N. J. Cowan, and D. L. Price. 1987. Neurofilament gene expression: a major determinant of axonal caliber. *Proc. Natl. Acad. Sci. USA.* 84:3472–3476.
Julien, J.-P., and W. E. Mushynski. 1982. Multiple phosphorylation sites in mammalian neurofilament polypeptides. *J. Biol. Chem.* 257:10467–10470.
Julien, J.-P., and W. E. Mushynski. 1983. The distribution of phosphorylation sites among identified proteolytic fragments of mammalian neurofilaments. *J. Biol. Chem.* 258:4019–4025.
Julien, J.-P., F. Cote, L. Beaudet, M. Sidky, D. Flavell, F. Grosveld, and W. Mushynski. 1987. Sequence and structure of the mouse gene coding for the largest neurofilament subunit. *Gene (Amst.).* 68:307–314.
Kaufman, E. K., K. Weber, and N. Geisler. 1985. Intermediate filament forming ability of desmin derivatives lacking either the amino-terminal 67 or the carboxy-terminal 27 residues. *J. Mol. Biol.* 185:733–742.
Klymkowsky, M. W., J. B. Bachant, and A. Domingo. 1989. Functions of intermediate filaments. *Cell Motil. Cytoskeleton.* 14:309–331.
Laemmli, U. K. 1970. Cleavage of structural proteins during the assembly of the head of bacteriophage T4. *Nature (Lond.).* 227:680–685.
Lee, V. M. Y., L. Otros, M. J. Carden, M. Hollosi, B. Dietzschold, and R. A. Lazzarini. 1988. Identification of the major multiphorylation site in mammalian neurofilaments. *Proc. Natl. Acad. Sci. USA.* 85:1998–2002.
Lees, J. F., P. S. Schneidman, S. F. Skuntz, M. J. Carden, and R. A. Lazzarini. 1988. The structure and organization of the human heavy neurofilament subunit NF-H. *EMBO (Eur. Mol. Biol. Organ.) J.* 7:1947–1958.
Lendahl, U., L. B. Zimmerman, and R. D. G. McKay. 1990. CNS stem cells express a new class of intermediate filament protein. *Cell.* 60:585–595.
Leonard, D. G. B., J. D. Gorham, P. Cole, L. A. Greene, and E. B. Ziff. 1988. A nerve growth factor-regulated messenger RNA encodes a new intermediate filament protein. *J. Cell Biol.* 106:181–193.
Levy, E., R. K. H. Liem, P. D'Eustacio, and N. J. Cowan. 1987. Structure and evolutionary origin of the gene encoding mouse NF-M, the middle molecular mass neurofilament protein. *Eur. J. Biochem.* 166:71–77.
Liem, R. K. H., and S. B. Hutchinson. 1982. Purification of individual components of the neurofilament triplet: filament assembly from the 70,000 dalton subunit. *Biochemistry.* 21:3221–3226.
Loewinger, L., and F. McKeon. 1988. Mutations in the nuclear lamin proteins resulting in their aberrant assembly in the cytoplasm. *EMBO (Eur. Mol. Biol. Organ.) J.* 7:2301–2309.
Lopata, M. A., and D. W. Cleveland. 1987. In vivo microtubules are copolymers of available β-tubulin isotypes: localization of each of six vertebrate β-tubulin isotypes using polyclonal antibodies elicited by synthetic peptide antigens. *J. Cell Biol.* 105:1707–1720.
Lopata, M. A., D. W. Cleveland, and B. Sollner-Webb. 1984. High level transient expression of a chloramphenicol acetyl transferase gene by DEAE-dextran mediated DNA transfection coupled with a dimethylsulfoxide or glycerol shock treatment. *Nucleic Acids Res.* 12:5707–5717.
Minami, Y., and H. Sakai. 1985. Dephosphorylation suppresses the activity of neurofilament to promote tubulin polymerization. *FEBS (Fed. Eur. Biochem. Soc.) Lett.* 185:239–242.
Monteiro, M. J., and D. W. Cleveland. 1989. Expression of NF-L and NF-M in fibroblasts reveals coassembly of neurofilament and vimentin subunits. *J. Cell Biol.* 108:579–593.
Munro, S., and H. R. B. Pelham. 1987. A C-terminal signal prevents secretion of luminal ER proteins. *Cell.* 48:899–907.
Myers, M. W., R. A. Lazzarini, V. M. Y. Lee, W. W. Schlaepfer, and D. L. Nelson. 1987. The human mid size neurofilament subunit: a repeated protein sequence and the relationship of its gene to the intermediate filament gene family. *EMBO (Eur. Mol. Biol. Organ.) J.* 6:1617–1626.
Napolitano, E. W., S. S. M. Chin, D. R. Colman, and R. K. H. Liem. 1987. Complete amino acid sequence and *in vitro* expression of rat NF-M, the middle molecular weight neurofilament protein. *J. Neurosci.* 7:2590–2599.
Ngai, J., T. R. Coleman, and E. Lazarides. 1990. Localization of newly synthesized vimentin subunits reveals a novel mechanism of intermediate filament assembly. *Cell.* 60:415–427.
Parysek, L. M., and R. D. Goldman. 1988. Distribution of a novel 57 kDa intermediate filament (IF) protein in the nervous system. *J. Neurosci.* 8:555–563.
Portier, M.-M., P. Brachet, B. Croizat, and F. Gros. 1984. Peripherin, a new member of the intermediate protein family. *Dev. Neurosci.* 6:335–344.
Sharp, G. A., G. Shaw, and K. Weber. 1982. Immunoelectron microscopical localization of the three neurofilament triple proteins along neurofilaments of cultured dorsal root ganglion neurons. *Exp. Cell Res.* 137:403–413.
Smith, P. K., P. I. Krohn, G. T. Hermanson, A. K. Mallia, F. H. Gartner, M. D. Provenzaus, E. K. Fujimoto, N. M. Goeke, B. J. Olson, and D. C. Klenk. 1985. Measurement of protein using bicinchoninic acid. *Anal. Biochem.* 150:76–85.
Steinert, P. M., and R. K. H. Liem. 1990. Intermediate filament dynamics. *Cell.* 60:521–523.
Steinert, P. M., and D. R. Roop. 1988. Molecular and cellular biology of intermediate filaments. *Annu. Rev. Biochem.* 57:593–625.
Steinert, P. M., R. H. Rice, D. R. Roop, B. L. Trus, and A. C. Steven. 1983. Complete amino acid sequence of a mouse epidermal keratin subunit and implications for the structure of intermediate filaments. *Nature (Lond.).* 302:794–800.
Sternberger, L. A., and N. M. Sternberger. 1983. Monoclonal antibodies distinguish phosphorylated and nonphosphorylated forms of neurofilaments in situ. *Proc. Natl. Acad. Sci. USA.* 80:6126–6130.
Steven, A., J. Hainfeld, B. L. Trus, J. S. Wall, and P. M. Steinert. 1983. Epidermal keratin filaments assembled in vitro have masses-per-unit-length that scale according to average subunit mass: structural basis for homologous packing of subunits in intermediate filaments. *J. Cell Biol.* 97:1939–1944.
Traub, P., and C. E. Vorgias. 1983. Involvement of the N-terminal polypeptide of vimentin in the formation of intermediate filaments. *J. Cell Sci.* 63:43–67.
Tokutake, S., R. K. H. Liem, and M. L. Shelanski. 1984. Each component of neurofilament assembles itself to make component-specific filament. *Biomed. Res.* 5:235–238.
van den Heuvel, R. M. M., G. J. J. M. van Eyes, F. C. S. Ramaekers, W. J. Quax, W. T. M. Vree Egberts, G. Schaart, T. M. Cuypers, and H. Bloemendal. 1987. Intermediate filament formation after transfection with modified hamster vimentin genes. *J. Cell Sci.* 88:475–482.